

Numerical Investigations of Mixing in Physically Heterogeneous Porous Media using the One- and Two-Particle Covariance

Anna M. Michalak and Peter K. Kitanidis

Department of Civil and Environmental Engineering, Stanford University, Stanford, California

In "Computational Methods in Water Resources XIII, Volume 1, Computational Methods for Subsurface Flow and Transport," pp. 423-429, edited by L.R. Bentley, J.F. Sykes, C.A. Brebbia, W.G. Gray and G.F. Pinder, A.A. Balkema, Rotterdam, The Netherlands, 2000.

ABSTRACT: Several works have pointed out that local dispersion plays a crucial role in determining the behavior of the concentration variance and coefficient of variation over time for conservative tracers. Numerical investigations aimed at evaluating the effect of the local dispersivity on dilution time scales are performed using a random-walk particle-tracking method model applied to transport of conservative solutes in representations of random media. The computed one- and two-particle covariances are used to characterize solute mixing by approximating the dilution time scales and the reactor ratios of the plumes. The effect of the microdispersivity on these time scales is found to be significant, with the time scales varying in an inverse fashion to the local dispersion coefficients. Dilution is found to vary with the diffusion time, with the dilution time scales being on the order of tens to thousands of diffusion times.

1 INTRODUCTION

Subsurface contamination by organic compounds is widespread, and has been the subject of numerous studies. The prediction of the location and extent of contaminant plumes, combined with the prediction of the rate at which the peaks of the concentration distribution attenuate over time, are issues of fundamental importance in hydrogeology. However, these predictive capabilities are limited, since the identification of field-scale mixing rates currently requires detailed field characterization.

The problem of field-scale spreading has been studied, particularly for the case where the velocity is a stationary random field (Dagan 1982, 1984, 1987, 1989, Gelhar & Axness 1983, Neuman et al. 1987). It has been demonstrated that the mean concentration in a stationary velocity field at large times satisfies an advection-dispersion equation with constant coefficients: the mean velocity and a constant macrodispersion tensor that dwarfs the local dispersion tensor. The behavior of the mean concentration has been studied extensively and is still receiving considerable attention. However, the mean concentration $\langle c \rangle$ is a smoothed version of the more variable concentration c . The concentration variance σ_c^2 , which is the mean square difference between the actual and the mean concentration, indicates how close the smooth mean concentration is to the more erratic actual one. Many upscaling methods assume that contaminant plumes

are smooth, whereas, in reality, the shape of plumes is highly irregular, and peak concentrations are much greater than those which would have been predicted using a Gaussian model. The degree to which predictions made using such an approach differ from observed conservative transport is the subject of this study.

Several works (Vomvoris & Gelhar 1990, Kapoor & Gelhar 1994a, b, Kapoor & Kitanidis 1996, 1998, Pannone & Kitanidis 1999) have pointed out that local dispersion plays a crucial role in determining the behavior of the concentration variance and coefficient of variation over time for conservative tracers. In particular, the time dependence of the concentration variance and dilution are functions of the ratio between the two-particle and one-particle covariances, where the two-particle covariance is the covariance tensor of the locations of two particles that start from the same point but follow different paths due to Brownian motion (Pannone & Kitanidis 1999). It has also been shown that the covariance of the centroid location is directly related to the two-particle covariance (Pannone & Kitanidis, in review). Therefore, the one- and two-particle covariances are important measures of mixing in a system. This paper examines the behavior of the one- and two-particle covariance as a function of time, in order to identify dilution time scales in heterogeneous formations. These time scales can then be used to model a plume's asymptotic approach

to the Gaussian shape. Specifically, this work focuses on the effect of the local dispersion coefficient on dilution time scales.

2 BACKGROUND

Consider transport of a conservative non-sorbing solute in a porous medium, described by the advection-dispersion equation,

$$\frac{\partial c}{\partial t} + \mathbf{u} \cdot \nabla c - \nabla \cdot (\mathbf{D} \nabla c) = 0 \quad (2.1)$$

where $c(\mathbf{x}, t)$ is the concentration at location \mathbf{x} and time t , $\mathbf{u} = \mathbf{u}(\mathbf{x}, t)$ is the advective velocity vector, and \mathbf{D} is the local dispersion tensor. Geologic formations being heterogeneous, the advective velocity is nonuniform in space. The variability in velocity \mathbf{u} , in conjunction with local dispersion, is primarily responsible for the spreading of solutes in geologic formations.

2.1 One- and two-particle covariances

The one-particle covariance is the tensor of the mean square deviation of the location of a single particle from its mean:

$$X_{ij} = \langle X'_i X'_j \rangle = \langle X_i X_j \rangle - \langle X_i \rangle \langle X_j \rangle \quad (2.2)$$

where X_i is the i^{th} coordinate of the particle position vector; the angle brackets indicate ensemble average, and $X'_i = X_i - \langle X_i \rangle$. The two-particle covariance is the covariance tensor of the locations of two particles that start from the same point but follow different paths due to Brownian motion:

$$\Theta_{ij} = \langle X'_i Y'_j \rangle = \langle X_i Y_j \rangle - \langle X_i \rangle \langle Y_j \rangle \quad (2.3)$$

where X indicates the coordinates of one particle and Y of the other.

2.2 Behavior of one- and two-particle covariances

The Lagrangian theory of Dagan (1984, 1989), tested through a series of numerical experiments by Bellin et al. (1992) and extended by Fiori (1996) to finite-Péclet cases, as well as the Eulerian theory of Gelhar & Axness (1983), predicts that the one-particle covariances increase linearly in time, at large times and in stationary formations.

Regarding the two-particle covariance, Pannone & Kitanidis (1999) suggested that Θ_{ij} should increase more slowly than X_{ij} , and may tend to become constant. Fiori & Dagan (pers. comm.) used small perturbation analysis to show that Θ_{11} increases logarithmically in 3-dimensional fields and with the square root of time in 2-dimensional fields. For parallel flow, Pannone & Kitanidis (1999) showed that Θ_{ij} tends to

a constant. Pannone & Kitanidis (in review) showed that, for periodic media, the two-particle covariance tends to a constant, and that the ensemble second spatial moment can be expressed as the difference between the one- and two-particle covariances. Since the ensemble second spatial moment is positive and increasing, it is clear that the one-particle covariance increases faster than the two-particle covariance. The larger the local dispersivities, the shorter the transient and the smaller the asymptotic two-particle covariance. However, the value of the macrodispersion coefficient remains practically the same, given the well-known insensitivity of macrodispersion coefficients to the value of local dispersion for large Péclet cases.

2.3 Two-particle correlation

At large times the correlation between the displacements in direction i of two particles that initially start at a single point gradually becomes proportional to $1/t$ because:

$$\rho_i(t) = \frac{\langle X'_i Y'_i \rangle}{\langle X'_i X'_i \rangle} \rightarrow \frac{\Theta_{ii}}{2D_{mii}t} \propto \frac{1}{t} \quad (2.4)$$

provided that Θ_{ii} tends to become constant.

Therefore, an important time scale is the time after which the two-particle correlation, ρ_i , becomes proportional to $\frac{1}{t}$. At this time, Θ_{ii} has become relatively constant, and \mathbf{D}_m has also stabilized. This time scale will be referred to as the two-particle correlation time scale, τ_ρ .

2.4 Coefficient of variation

At large time, when the covariance is equal to $2\mathbf{D}_m t$ and the cross covariance between \mathbf{X} and \mathbf{Y} is time invariant, the coefficient of variation at the plume centroid ($\mathbf{x} = \mathbf{U}_m t$, where \mathbf{U}_m is the mean seepage velocity) is proportional to t^{-1} at the lowest order approximation, and goes as (Kapoor & Gelhar 1994a, b, Pannone & Kitanidis 1999):

$$Cv \simeq \frac{\tau_d}{t} \quad (2.5)$$

where, if \mathbf{D}_m and Θ_{ii} are diagonal,

$$\tau_d = \sqrt{\frac{1}{8} \left[\left(\frac{\Theta_{11}}{D_{m11}} \right)^2 + \left(\frac{\Theta_{22}}{D_{m22}} \right)^2 \right]} \quad (2.6)$$

for a 2-dimensional domain. The larger the coefficient of variation time scale, τ_d , the longer it takes for small-scale fluctuations to attenuate and for a plume in a given realization to approach the mean concentration. Therefore, τ_d controls the rate at which a plume tends to become Gaussian.

If the microdispersivity is increased, the longitudinal macrodispersion coefficient will remain unchanged. However, according to Kapoor & Gelhar (1994a, b) and Pannone & Kitanidis (1999), the value of τ_d should decrease when the microdispersivity is increased. The effect of the increase in the microdispersivity on the transverse macrodispersion coefficient can also affect τ_d , in cases where the magnitude of Θ_{22} is nonzero.

2.5 Dilution index and reactor ratio

The dilution index is a measure of the volume occupied by the solute (Kitanidis 1994). Assuming that the concentration is normalized to unit mass, the dilution index is expressed by:

$$E(t) = \exp \left[- \int c(\mathbf{x}, t) \ln(c(\mathbf{x}, t)) d\mathbf{x} \right] \quad (2.7)$$

where the integral is over the whole domain. The reactor ratio, a dimensionless measure of degree of dilution that takes values between 0 and 1, is defined as (Kitanidis 1994):

$$M = \frac{E(t)}{E_{\max}(t)} \quad (2.8)$$

where

$$E_{\max} = \exp \left[- \int \hat{c}(\mathbf{x}, t) \ln \hat{c}(\mathbf{x}, t) d\mathbf{x} \right] \quad (2.9)$$

where \hat{c} is a spatial concentration distribution that maximizes $E(t)$ for a given domain and time. In many cases, the distribution that maximizes the dilution index is a Gaussian concentration profile. In this case, the reactor ratio measures how close to a Gaussian the actual plume is; the plume tends to become Gaussian when $M(t)$ tends to become 1.

At large time ($t \gg \tau_\rho$), the geometric mean of the reactor ratio is (Kapoor & Kitanidis 1996, 1998):

$$\begin{aligned} M_g(t) &= \exp[\langle \ln M(t) \rangle] \\ &\simeq \exp \left[- \frac{1}{2} \int \frac{\sigma_c^2}{\langle c \rangle} dx \right] \end{aligned} \quad (2.10)$$

where, it can be shown (Pannone & Kitanidis 1999) that, when \mathbf{D}_m and Θ_{ii} have reached their time invariant values,

$$\int \frac{\sigma_c^2}{\langle c \rangle} dx = \frac{1}{2} Tr(\Theta \mathbf{D}_m^{-1}) \frac{1}{t} \quad (2.11)$$

Thus:

$$M_g(t) \simeq \exp \left[- \frac{1}{4} Tr(\Theta \mathbf{D}_m^{-1}) \frac{1}{t} \right] \quad (2.12)$$

We see that there is a characteristic time associated with dilution,

$$\kappa = \frac{1}{4} Tr(\Theta \mathbf{D}_m^{-1}) \quad (2.13)$$

In the special case that \mathbf{D}_m is diagonal and the only nonzero element of Θ_{ii} is Θ_{11} ,

$$\kappa = \frac{1}{4} \frac{\Theta_{11}}{D_{m11}} \quad (2.14)$$

Thus the ratio of the time-invariant Θ_{ii} to macrodispersion coefficients controls the rate of dilution. However, it is worth noting that $\exp(-\kappa/t)$ converges toward 1 slowly, and it is required that $t \gg \kappa$ for the plume to approach a Gaussian distribution. As with τ_d , a change in the microdispersivity should result in a decrease in κ (Pannone & Kitanidis 1999, in review).

3 NUMERICAL METHOD

The following section is broken up into the three steps involved in the performed simulations: field generation, flow solution, and conservative transport.

3.1 Field generation

The two-dimensional conductivity field used in this work was generated using a numerical spectral approach. The numerical method yields a periodic cell of specified dimensions and heterogeneity statistics. A Gaussian covariance function was used for the domain. The method used for generating these domains is based on the work of Van Lent & Kitanidis (1989), Van Lent (1992), and Dykaar & Kitanidis (1992a). The effective conductivity and log-conductivity variance of the resulting field are computed according to the method described in Dykaar & Kitanidis (1992a).

3.2 Flow solution

The flow solution is obtained by solving an elliptic partial differential equation with non-constant coefficients and forcing function. A hydraulic head gradient is imposed over a periodic cell, with periodic boundary conditions in both directions. The method is described in detail in Dykaar & Kitanidis (1992a, b).

The method is extended for this application since using this velocity solution directly would not ensure mass conservation at the grid scale. Therefore, the stream function solution is needed, which allows for the calculation of exact fluxes normal to the element boundaries, thereby ensuring local mass conservation. The streamfunction solution is obtained as described in Michalak & Kitanidis (in prep.).

Using the velocity solution obtained from the stream function solution by linear interpolation results in ideal mass conservation for each grid element.

Therefore, linear interpolation is performed in the x_1 -direction for u_1 , and in the x_2 -direction for u_2 .

3.3 Conservative transport

A random-walk particle tracking scheme is used for transport simulations. The scheme uses a constant local dispersion coefficient, and a semi-analytical method for advection. The random-walk particle tracking routine is implemented using the stream function solution. The semi-analytical computation of path lines developed by Pollock (1988) is then applied. This method allows for the analytical determination of particle positions within grid cells when linear interpolation is used for the velocities within each grid cell. This scheme, combined with using the stream function solution, allows for stream function value conservation for each particle, in the absence of local dispersion. In other words, particles remain on their initial streamlines exactly, unless dispersive processes are applied. In short, numerical dispersion is entirely eliminated.

The microdispersion step was performed as follows:

$$\mathbf{X}(t + \Delta t) = \mathbf{X}(t) + \mathbf{Z}(2\mathbf{D}\Delta t)^{1/2} \quad (3.4)$$

where \mathbf{X} is a vector of a particle's coordinates, Δt is the time step, and \mathbf{Z} is a vector of normally distributed random numbers with a mean of 0, and a variance of 1.

The initial condition for the transport simulations is a uniform distribution of particles within a single periodic cell, with two particles starting from each position. Such an initial condition allows one to obtain a spatial average of the evolution of the one- and two-particle covariance while performing a single simulation.

The one-particle covariance is calculated according to:

$$X_{ij}(t) = \frac{1}{N_p} \sum_1^{N_p} \begin{bmatrix} X_i - X_{0i} - U_{mi}t \\ X_j - X_{0j} - U_{mj}t \end{bmatrix} \quad (3.5)$$

where X_{0i} indicates the initial position of each particle, and N_p is the total number of particles. The two-particle covariance is calculated according to:

$$\Theta_{ij}(t) = \frac{2}{N_p} \sum_1^{N_p/2} \begin{bmatrix} (X_i - X_{0i} - U_{mi}t) \\ (Y_j - Y_{0j} - U_{mj}t) \end{bmatrix} \quad (3.6)$$

where X_i and Y_i indicate the coordinates of two particles that started at the same location, and, therefore, $X_{0i} = Y_{0i}$. These formulations were selected to minimize numerical error. For the simulations performed, X_{ij} and Θ_{ij} are diagonal, since the coordinate system is aligned with the principal axes of anisotropy.

Table 1: Domain specifications

| Parameter | Symbol | Value |
|---------------------------|-------------------------------------|--------------|
| Periodic cell length | Lx_1 | 20 m |
| | Lx_2 | 1 m |
| Number of nodes | Nx_1 | 1024 |
| | Nx_2 | 1024 |
| Integral scale | lx_1 | 0.125 m |
| | lx_2 | 0.00625 m |
| Porosity | n | 0.3 |
| Hydraulic conductivity | \overline{K} | 0.0001 m/s |
| Log-conductivity variance | σ_Y^2 | 0.32 |
| Mean head gradient | $\frac{\partial\phi}{\partial x_1}$ | 1.00 $e - 3$ |

4 RESULTS AND DISCUSSION

The simulations performed as part of this work are aimed at investigating the effect of the local dispersivity on the dilution time scales. The resulting rate of approach to a gaussian plume, as measured by the reactor ratio, is also determined. The domain specifications used for the simulations are presented in Table 1, and the microdispersivity used ranges from 0.001 to 0.005 m . For simplicity, the microdispersivity was kept isotropic for all simulations. This is justified since the value of the longitudinal microdispersivity is not expected to have a major effect on the macrodispersion parameters. Furthermore, microdispersivities used are on the order of molecular diffusion, which acts evenly in all directions. These parameter values were selected based on previous work, which determined domain size and discretization requirements for proper representation of stationary heterogeneous formations using a periodic approach (Michalak & Kitanidis, in prep.). All simulations were performed using 100,000 particles starting at 50,000 distinct initial positions.

4.1 Two-particle correlation time scale

A typical plot of the longitudinal two-particle correlation as a function of diffusion time is presented in cartesian coordinates in Figure 1, and in logarithmic coordinates in Figure 2 for the case $\alpha = 0.001 m$. The transverse cross-covariance Θ_{22} was found to be essentially zero for all cases examined, and, therefore, only longitudinal results are presented herein. The plots are presented with time non-dimensionalized by the transverse diffusion time $ly^2/(U_{m1}\alpha)$, since this time has been suggested to be an important parameter in quantifying subsurface mixing (Kitanidis 1992, Kapoor & Kitanidis 1996). As can be seen from Figures 1 and 2, the behavior of the two-particle correlation is fairly smooth, even at small times. At early times, the two-particle correlation ρ_1 decreases with $t^{-1/2}$. The two-particle correlation becomes propor-

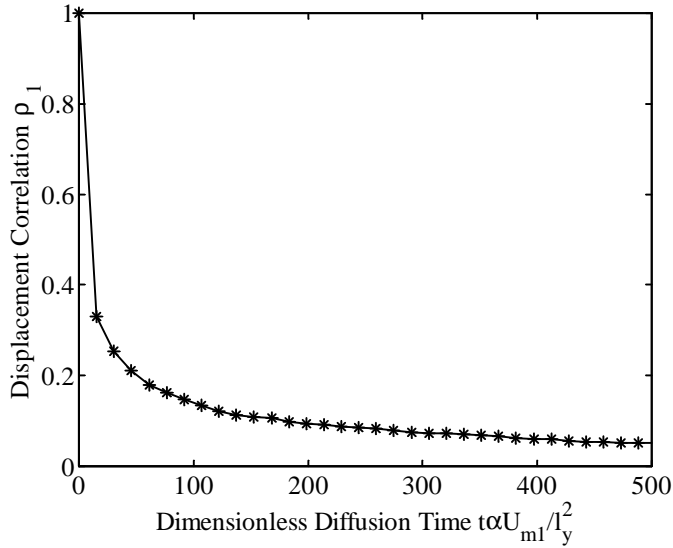


Figure 1: Two-particle correlation as a function of transverse diffusion time

tional to $\frac{1}{t}$ when the slope of the two-particle correlation as a function of time becomes -1 in logarithmic coordinates. This time scale, termed two-particle correlation time scale, τ_ρ , is the time scale after which the large time approximations for the coefficient of variation time scale, τ_d , and the reactor ratio, M_g , become valid. The required diffusion time for the two-particle correlation to become proportional to $\frac{1}{t}$ for the case presented in Figures 1 and 2 is about 2100. It should be noted that, for the case examined, this time scale corresponds to a travel time of over 7 years.

Table 2 presents the two-particle correlation time scale, τ_ρ , in terms of diffusion times as a function of microdispersivity. As seen in Table 2, this time scale is on the order of a thousand diffusion times. The

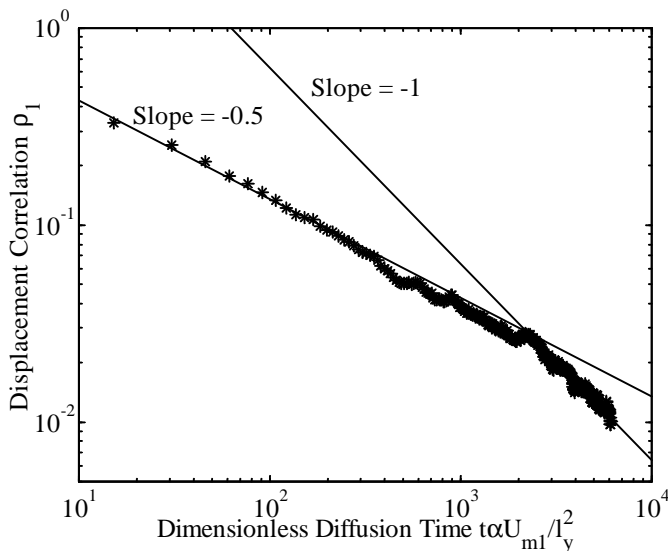


Figure 2: Two-particle correlation as a function of transverse diffusion time

Table 2: Dilution time scales as a function of microdispersivity

| α [m] | $\tau_\rho \frac{\alpha U_{m1}}{l_y^2}$ | $\tau_d \frac{\alpha U_{m1}}{l_y^2}$ | $\kappa \frac{\alpha U_{m1}}{l_y^2}$ |
|--------------|---|--------------------------------------|--------------------------------------|
| 0.001 | 2100 | 44 | 31 |
| 0.002 | 1300 | 32 | 23 |
| 0.003 | 1000 | 41 | 29 |
| 0.004 | 1000 | 34 | 24 |
| 0.005 | 1000 | 37 | 26 |

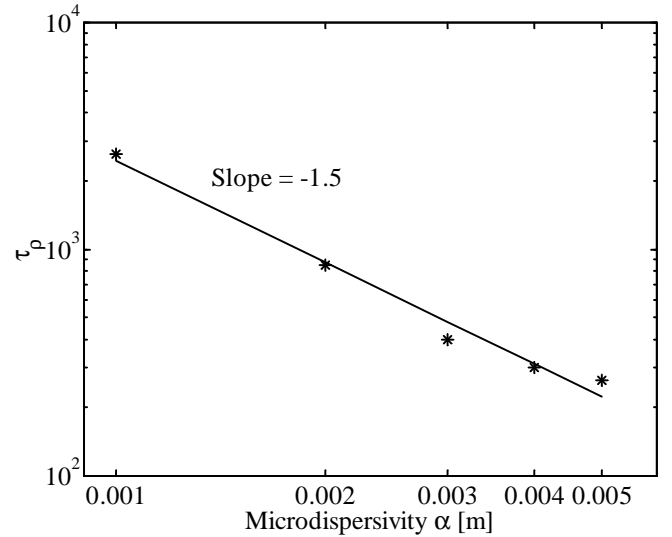


Figure 3: Two-particle correlation time scale as a function of microdispersivity

effect of the local dispersion coefficient on τ_ρ is presented in Figure 3. As seen in this figure, the two-particle correlation time scale varies inversely with the local dispersivity. The time scale τ_ρ goes as:

$$\tau_\rho \simeq \frac{1}{\alpha^{1.5}} \quad (4.1)$$

Although some dependence on the local dispersivity had been predicted (Pannone & Kitanidis, in review), the results of this study show that this dependence is very strong, with more than a proportional decrease in τ_ρ for an increase in α . It would be expected that, for large values of log-conductivity variance, the decrease in τ_ρ as a function of α may be even more pronounced, since high heterogeneity may contribute to a nonlinear increase in the rate of mixing, and, therefore, a decrease in the time required to achieve a two-particle correlation proportional to $\frac{1}{t}$.

Therefore, the local dispersion is an extremely important parameter for dilution estimation, despite the fact that it has no effect on the longitudinal macrodispersion coefficient. This fact clearly demonstrates that, although macrodispersion theories give good indications of the rate of spread of plumes, actual dilu-

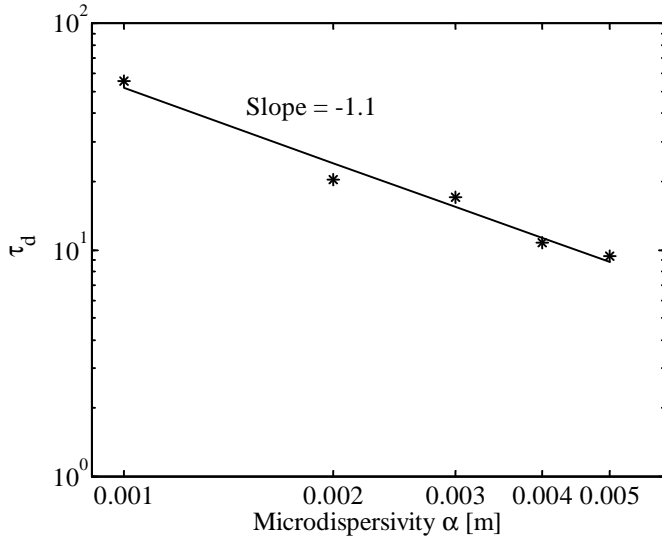


Figure 4: Coefficient of variation time scale as a function of microdispersivity

tion is controlled by a different set of parameters, and can require significantly longer time scales.

4.2 Coefficient of variation time scale

After time τ_ρ , Θ_{11} and \mathbf{D}_m are essentially constant. Therefore, the coefficient of variation time scale, τ_d , can be determined as:

$$\tau_d = \frac{\sqrt{2}}{4} \frac{\Theta_{11}}{D_{m11}} \quad (4.2)$$

Table 2 presents the coefficient of variation time scale, τ_d , in terms of diffusion times as a function of microdispersivity. As seen in Table 2, this time scale is on the order of tens of diffusion times. The effect of the local dispersion coefficient on this time scale is also presented in Figure 4. As seen in this figure, this time scale also varies in an inverse fashion with the local dispersion, as predicted by Kapoor & Gelhar (1994a, b) and Pannone & Kitanidis (1999). The coefficient of variation time scale goes as:

$$\tau_d \simeq \frac{1}{\alpha^{1.1}} \quad (4.3)$$

Furthermore, as with τ_ρ , large log-conductivity variance values could contribute to an even stronger dependence on the local dispersion, due to the nonlinearly enhanced mixing due to heterogeneity.

It should be noted that, for the domain setup used for these simulations, the longitudinal macrodispersion coefficient is, in some cases, of the same order of magnitude as the microdispersivity. This is due to the small integral scales used in the domain. Therefore, for the larger microdispersivities, the longitudinal macrodispersion was affected by changes in the

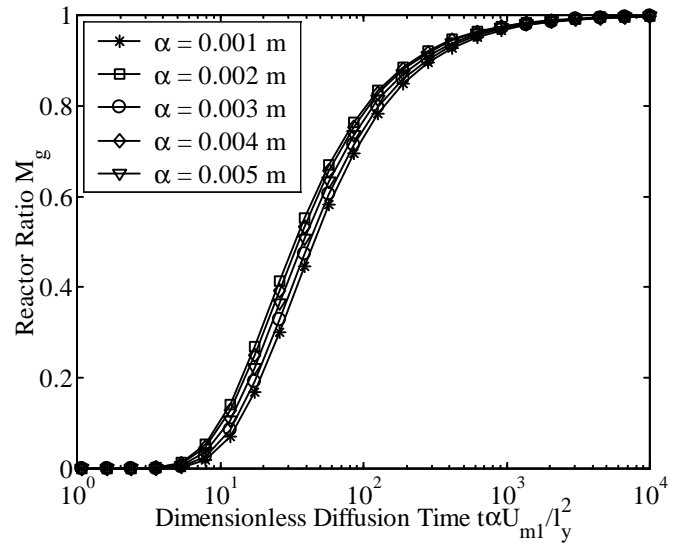


Figure 5: Large time geometric mean of reactor ratio as a function of transverse diffusion time

microdispersivity, which is contrary to results predicted by linear theory. This type of effect is not observed when smaller microdispersivities or larger integral scales are used. If this variation had been ignored, and a constant value used for D_{m11} , the inverse relation between τ_d and α would have been even more pronounced, with τ_d varying proportionally to $\alpha^{-1.5}$.

4.3 Reactor ratio

Once Θ_{11} and \mathbf{D}_m have stabilized to time invariant values, the geometric mean of the reactor ratio becomes:

$$M_g(t) \simeq \exp\left[-\frac{\kappa}{t}\right] \quad (4.4)$$

Table 2 presents the reactor ratio time scale, κ , in terms of diffusion times as a function of microdispersivity. The reactor ratio for various values of the local dispersion coefficient is presented in Figure 5 as a function of the time non-dimensionalized by the transverse diffusion time. It is important to note that this relation is only valid at large times, and will therefore apply starting at a nonzero reactor ratio and time. However, since the actual time and corresponding reactor ratio at which this relation begins to be applicable is realization and initial plume shape dependent, such results are not presented. Figure 5 should be interpreted as an indication of the large-time behavior of the reactor ratio, and not as a strict correspondence between a given time and reactor ratio value.

As can be seen from Figure 5, although the time scale κ for the reactor ratio's approach to unity is relatively small, the convergence of the reactor ratio to unity takes thousands of diffusion times. Therefore, for the vast majority of contaminant plumes, a Gaussian assumption is unjustified.

5 CONCLUSIONS

The time scale required for the two-particle correlation to become inversely proportional to time, τ_ρ , is on the order of a thousand transverse diffusion times. This time scale is strongly affected by local dispersion, and varies inversely with the microdispersivity.

The time scale associated with the decay of the coefficient of variation at the plume centroid, τ_d , is on the order of tens of transverse diffusion times. However, despite this relatively short time scale, a plume's approach to a Gaussian shape, as represented using the reactor ratio, requires thousands of diffusion times. This time scale also varies inversely with the local dispersion.

Therefore, the ensemble macrodispersion coefficient may reach its asymptotic value well before the concentration variance decays, demonstrating that dilution in subsurface environments is extremely slow relative to dispersion. Therefore, for the majority of practical applications, the assumption of a Gaussian plume is a gross oversimplification.

6 ACKNOWLEDGMENTS

Funding for this study was provided by a Stanford Graduate Fellowship for Anna M. Michalak, and by the National Science Foundation under project EAR-9522651, "Factors Affecting Solute Dilution in Heterogeneous Formations". The views presented in this paper do not necessarily reflect those of Stanford University or of the National Science Foundation.

REFERENCES

- Bellin, A., Salandin, P. and Rinaldo, A., 1992. Simulation of Dispersion in Heterogeneous Porous Formations: Statistics, First-Order Theories, Convergence of Computations. *Water Resources Research*, 28(9): 2211-2227.
- Dagan, G., 1982. Stochastic modeling of groundwater flow by unconditional and conditional probabilities 1. Conditional simulations and the direct problem. *Water Resources Research*, 18(4): 813-833.
- Dagan, G., 1984. Solute transport in heterogeneous porous formations. *Journal of Fluid Mechanics*, 145: 151-177.
- Dagan, G., 1987. Theory of solute transport by groundwater. *Annual Review of Fluid Mechanics*, 19: 183-215.
- Dagan, G., 1989. *Flow and transport in porous media*. Springer-Verlag, 465 pp.
- Dykaar, B.B. and Kitanidis, P.K., 1992a. Determination of the Effective Hydraulic Conductivity for Heterogeneous Porous Media Using a Numerical Spectral Approach 1. Method. *Water Resources Research*, 28(4): 1155-1166.
- Dykaar, B.B. and Kitanidis, P.K., 1992b. Determination of the Effective Hydraulic Conductivity for Heterogeneous Porous Media Using a Numerical Spectral Approach 2. Results. *Water Resources Research*, 28(4): 1167-1178.
- Fiori, A., 1996. Finite Peclet extensions of Dagan's solutions to transport in anisotropic heterogeneous formations. *Water Resources Research*, 32(1): 193-198.
- Gelhar, L.W. and Axness, C.L., 1983. Three-Dimensional Stochastic Analysis of Macrodispersion in Aquifers. *Water Resources Research*, 19(1): 161-180.
- Kapoor, V. and Gelhar, L.W., 1994a. Transport in three-dimensionally heterogeneous aquifers: 1. Dynamics of concentration fluctuations. *Water Resources Research*, 30(6): 1775-1788.
- Kapoor, V. and Gelhar, L.W., 1994b. Transport in three-dimensionally heterogeneous aquifers: 2. Predictions and observations of concentration fluctuations. *Water Resources Research*, 30(6): 1789-1801.
- Kapoor, V. and Kitanidis, P.K., 1996. Concentration fluctuations and dilution in two-dimensionally periodic heterogeneous porous media. *Transport in Porous Media*, 21(1): 91-119.
- Kapoor, V. and Kitanidis, P.K., 1998. Concentration fluctuations and dilution in aquifers. *Water Resources Research*, 34(5): 1181-1193.
- Kitanidis, P.K., 1992. Analysis of macrodispersion through volume-averaging: Moment equations. *Stochastic Hydrology and Hydraulics*, 6: 5-25.
- Kitanidis, P.K., 1994. The concept of the dilution index. *Water Resources Research*, 30(7): 2011-2026.
- Michalak, A. M. and Kitanidis, P. K. in prep. An Improved Numerical Method for Mixing in Physically Heterogeneous Media
- Neuman, S.P., Winter, C.L. and Newman, C.M., 1987. Stochastic Theory of Field-Scale Fickian Dispersion in Anisotropic Porous Media. *Water Resources Research*, 23(3): 453-466.
- Pannone, M. and Kitanidis, P.K., 1999. Large-time behavior of concentration variance and dilution in heterogeneous formations. *Water Resources Research*, 35(3): 623-634.
- Pannone, M. and Kitanidis, P.K., In review. Analysis with the Method of Moments of Dispersion and Dilution in Heterogeneous Velocity Fields. *Water Resources Research*.
- Pollock, D.W., 1988. Semianalytical Computation of Path Lines for Finite-Difference Models. *Ground Water*, 26(6): 743-750.
- Van Lent, T. and Kitanidis, P.K., 1989. A numerical spectral approach for the derivation of piezometric head covariance functions. *Water Resources Research*, 25(11): 2287-2298.
- Van Lent, T.J., 1992. *Numerical Spectral Methods Applied to Flow in Highly Heterogeneous Aquifers*. Ph. D. Thesis, Stanford University, Civil Eng.
- Vomvoris, E.G. and Gelhar, L.W., 1990. Stochastic analysis of the concentration variability in a three-dimensional heterogeneous aquifer. *Water Resources Research*, 26(10): 2591-2602.